Informatics in Medicine Unlocked 19 (2020) 100335

Contents lists available at ScienceDirect

Informatics in Medicine Unlocked

journal homepage: http://www.elsevier.com/locate/imu

Spark Architecture for deep learning-based dose optimization in medical imaging

Clémence Alla Takam [a], Odette Samba [a,b], Aurelle Tchagna Kouanou [a,c,*], Daniel Tchiotsop [d]

[a] Unité de Recherche de Matière Condensée d'Electronique et de Traitement du Signal (URMACETS), Faculty of Science, University of Dschang, P.O.Box 67, Dschang, Cameroon
[b] Service de Radiothérapie, Hôpital Général de Yaoundé-Cameroun, Cameroon
[c] Department of Training, Research, Development and Innovation, InchTech's Solutions, Yaounde, Cameroon
[d] Unité de Recherche d'Automatique et d'Informatique Appliquée (URAIA), IUT-FV de Bandjoun, Université de Dschang-Cameroun, B.P. 134, Bandjoun, Cameroon

ARTICLE INFO

Keywords:
Computer tomography scan image
Deep learning
Spark framework
Architecture
Low dose optimization

ABSTRACT

Background and objectives: Deep Learning (DL) and Machine Learning (ML) have brought several breakthroughs to biomedical image analysis by making available more consistent and robust tools for the identification, classification, reconstruction, denoising, quantification, and segmentation of patterns in biomedical images. Recently, some applications of DL and ML in Computed Tomography (CT) scans for low dose optimization were developed. Nowadays, DL algorithms are used in CT to perform replacement of missing data (processing technique) such as low dose to high dose, sparse view to full view, low resolution to high resolution, and limited angle to full angle. Thus, DL comes with a new vision to process biomedical data imagery from CT scan. It becomes important to develop architectures and/or methods based on DL algorithms for minimizing radiation during a CT scan exam thanks to reconstruction and processing techniques.
Methods: This paper describes DL for CT scan low dose optimization, shows examples described in the literature, briefly discusses new methods used in CT scan image processing, and offers conclusions. We based our study on the literature and proposed a pipeline for low dose CT scan image reconstruction. Our proposed pipeline relies on DL and the Spark Framework using MapReduce programming. We discuss our proposed pipeline with those proposed in the literature to conclude the efficiency and importance.
Results: An architecture for low dose optimization using CT imagery is suggested. We used the Spark Framework to design the architecture. The proposed architecture relies on DL, and permits us to develop efficient and appropriate methods to process dose optimization with CT scan imagery. The real implementation of our pipeline for image denoising shows that we can reduce the radiation dose, and use our proposed pipeline to improve the quality of the captured image.
Conclusion: The proposed architecture based on DL is complete and enables faster processing of biomedical CT imagery as compared with prior methods described in the literature.

1. Introduction

Machine Learning (ML) techniques are broadly used in biomedical imaging research in the form of many successful clustering and classifier algorithms. ML is a branch of artificial intelligence (AI) that has been employed in a variety of applications. It is used to analyze complex data sets and find patterns and relationships among such data without being explicitly programmed [1]. ML techniques are essential components of research in medical imaging. Recently, a highly flexible ML approach known as Deep Learning (DL) has emerged as a technology to improve the performance of existing ML techniques and to solve previously intractable problems [2]. DL has emerged from the ML and computer vision communities [3]. The key to the success of methods based on DL is its independence from explicit imaging models, backup by big domain-specific data, and the image quality is optimized by learning features in an end-to-end manner [4]. It has been recently applied to problems of Natural Language Processing, Face Recognition, Voice Recognition, Image Classification, and Automatic Diagnosis, with good results [3,5–8]. Nowadays, DL has allowed many applications in (CT), and helps to enhance the speed of interpretation, diagnostic accuracy,

* Corresponding author. Unité de Recherche de Matière Condensée d'Electronique et de Traitement du Signal (URMACETS), Faculty of Science, University of Dschang, P.O.Box 67, Dschang, Cameroon.tkaurelle@gmail.com

https://doi.org/10.1016/j.imu.2020.100335
Received 24 December 2019; Received in revised form 12 April 2020; Accepted 24 April 2020
Available online 30 April 2020

and clinical efficiency. Moreover, CT is broadly used in detection, diagnosis, and image-guided therapy for both research purposes and clinical [9–12]. CT is a well-known imaging technique that allows for non-invasive visualization of the interior of an object [13]. The main problem in CT scans is optimization and minimization of radiation dose during an exam, especially in the pediatric cranial scan. Developing and optimizing dosimetry protocols in the pediatric cranial scan is of great interest in the worldwide healthcare community. Indeed, patient-specific dosimetry is of significant interest in pediatric cranial applications, as radiation sensitivity is outstandingly higher compared to adults. This is because children have a higher risk to develop cancer compared to adults receiving the equivalent dose [14]. Given the possible risk of X-ray radiation to pediatric patients, low-dose CT has aroused considerable interest in the biomedical imaging field [15]. However, the main issue in low-dose CT is the image noise and quality of obtained results. To overcome drawbacks, DL with Convolutional Neural Network (CNN) algorithms are used. Indeed, one of the goals of various DL and ML algorithms are to improve consistency, quality, and/or aptness of data interpretation in diagnostics. DL can improve then image quality during low-dose CT cranial scanning.

In this paper, we focus mainly on dose optimization in pediatric cranial scan using CNN for DL along with image processing. We present a pipeline that describes the optimal algorithms and methods drawn from the literature. The pipeline performs the steps of image denoising, image splitting, CNN, image retrieval, image diagnosis and storage. We describe the importance to use a big data Framework (Spark) with the MapReduce method to build our proposed architecture. We discuss our proposed pipeline and architecture with those described in the literature. The implementation of our FCNN is performed. The remainder of the work is organized as follows: section 2 presents the state-of-the-art of published works in the field. In section 3, these works are theoretically exploited and our proposed architecture is presented. Section 4 presents implementation of our architecture and obtained results. Results are examined and discussed in section 5. Section 6 provides a conclusion and future works.

2. State-of-the-art

ML and DL are becoming established disciplines in the broad field of AI in analyzing and utilizing patterns in datasets [16–19]. DL models such as CNN refer to a class of computing machinery that can learn a hierarchy of features by constructing high-level attributes from low-level ones, thus automating the process of feature builder [8,20,21]. In the CT scan image, DL is often used for the purpose of minimizing radiation exposure, noisier images, and CT image reconstruction. CT uses gamma rays, X-rays, ultrasonic waves, or other types of beams in concert with susceptible detectors to sequentially scan individual parts of the human body [22]. However, for CT scanning, obtaining of excellent image quality entails a radiation dose very high during the procedure.

Furthermore, patient-specific dosimetry is of high interest in pediatric cranial applications, as radiation sensitivity is noteworthily higher as compared to adults [23]. Hence, low dose CT is essential in these conditions. Low-dose CT biomedical imaging techniques have been a focus over the past several years to alleviate concerns about patient exposure to X-ray radiation coupled with broadly used CT scans [24]. According to Ref. [23], where the authors review in 2018 the dosimetry applications in pediatric diagnostic methods, including CT and nuclear medicine applications, there are three critical challenges to address for dose optimization in the pediatric cranial scan:

- The computation time and the need for computing resources for implementing massive, accurate, and realistic MC simulations incorporating patient-specific characteristics.
- Validation of several clinical protocols used in pediatric therapy and diagnosis is based on real data.
- There are typical difficulties in applying experimental dosimetry during clinical practice on children (such as the CT dosimetry based TLDs at the body surface).

Based on these challenges, many works are performed to reduce radiation dose and to maintain the quality of the captured image during the CT exam. In Ref. [25–31], the authors proposed new methods to optimize dose during CT scanning. However, decreasing radiation can lead to decreased image quality. DL can be used to overcome this problem by reconstruction, and prevent removal of useful information from the original CT image. Many types of research and publications have been described in the literature. To reduce radiation dose, some works were based on traditional methodology (protocol optimization) and others were based on DL and ML techniques. In Ref. [32–35], the author proposed methods to optimize radiation dose were based on studies of protocol used. Dalmazo et al. in Ref. [36] performed a survey of radiation dose in CT protocols with phantoms and ionization chambers at a university hospital. Their study was based only on an equipment investigation. In 2012, Dougeni et al. reviewed patient dose and optimization procedures in adult and pediatric CT scanning [37]. They discussed and compared many kinds of literary works in dose optimization in CT. Recently, in 2019, Smith-Bindman et al. performed a multicenter study consisting of 151 institutions across seven countries, and from over 2.0 million CT examinations of adults, proposed a practical protocol to optimize dose radiation during a CT scanning or other radiological examination [38]. In 2020 Abdukkadir et al. performed a study to optimize the current local practice through investigation of radiation dose distribution and existing routine scanning protocols for head and abdomen pediatric CT examinations at the Kelanta Radiology Department in Malaysia [39]. Also, Choi et al. in Ref. [40], proposed a work to optimize dose and image quality with various exposure conditions and phantom diameters in a pediatric abdominal CT scan. In Ref. [41], the authors assessed image quality of dose-optimized (DO) C-spine CT in patients capable of shoulder pull-down in an emergency setting, to reduce the exposure dose and improve image quality. Chen et al., in 2017, determined how image quality after CT scan can be improved [42]. Currently, many works are based on DL or ML to see how to reduce the radiation dose during a CT scan exam and maintain satisfactory resolution and quality of captured image.

Concerning ML and DL in dose optimization, Kang et al. proposed in 2017 an algorithm which uses CNN applied to the windowed Fourier transform (wavelet transform) coefficients of low-dose CT images. Their CNN is constructed with a residual learning architecture for faster network training and better performance. The execution of their proposed algorithm showed the effective elimination of complex noise patterns from CT images derived from a reduced X-ray dose, and the wavelet-domain CNN was efficacious when used to dampen noise from low-dose CT [43]. Jung et al. also performed in 2017 a survey of recent applications of DL in the analysis of CT and magnetic resonance imaging (MRI) biomedical images in a range of tasks and target organs, and they concentrated on the improvement of accuracy and the productivity of current diagnostic analysis [44]. They introduced some promising applications that significantly changed the current pipeline of biomedical imaging [44]. However, they did not provide a workflow for their introduced methods. Xuy et al. in Ref. [45] proposed a DL method to resolve the issue of quality of PET image reconstruction for excellent clinical diagnosis when the radiation dose is low during the capture of the biomedical image via PET scan [45]. They basis was an encoder-decoder residual deep network with concatenating skip connections. Liu et al. evaluated how to perform noise reduction and image quality (IQ) enhancement using a DL-based optimization algorithm for low-dose coronary CT angiography (CCTA) [46].

A new DL framework for 3-D CT reconstruction is presented in Ref. [47] by Wurfl et al. They proposed a new type of cone-beam back-projection layer, efficiently calculating the forward pass and their framework allowed joint optimization of correction steps in the

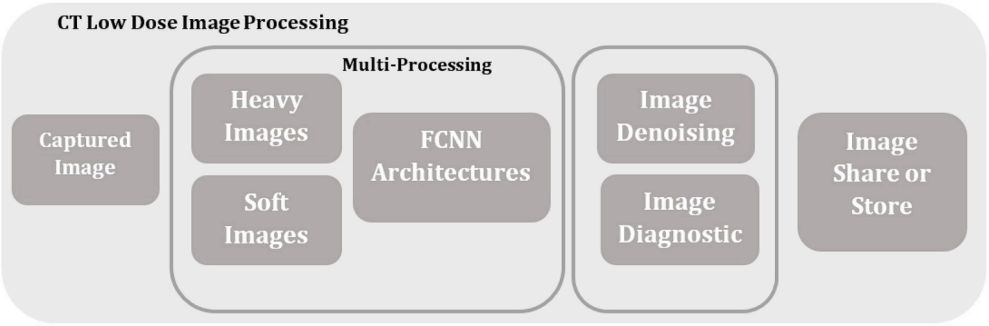

Fig. 1. Pipeline for low dose CT image reconstruction. Only the multi-processing step will be designed with the Spark framework.

volume and projection domain. Despite the promising performance, their methods are limited to post-processing. Shan et al. introduced in 2018 a Conveying Path based Convolutional Encoder-decoder (CPCE) network in 2D and 3D configurations within the Generative Adversarial Network (GAN) framework for low-dose CT denoising based on transfer learning [48]. Tian et al. utilized CNN and combined two networks to increase the width of the network, and thus obtained more features. This allowed them to design a novel network termed a batch-renormalization denoising network (BRDNet), to remove image noise [49]. However, the authors did not use CT imagery. Lee et al. developed a method using DL with its CNN that allowed analysis of CT image tasks, such as object detection and semantic segmentation, or to test other biomedical imaging modalities such as MRI and positron emission tomography (PET) [50]. However, their methods weren't based on low dose CT. You et al. in 2018 presented a semi-supervised deep learning approach to accurately recover high-resolution (HR) CT imagery from low resolution (LR) counterparts to bring superior diagnostic quality, which is consistent with systematic quantitative evaluations in terms of traditional image quality measures [4]. In their deep imaging process, they incorporated residual learning, CNN, and network-in-network techniques for feature restoration and extraction. Recently, in 2019, Gu et al. combined a random forest with coupled dictionary learning to reduce CT scan radiation while ensuring a new low-dose CT super-resolution reconstruction and CT image quality by using an ML algorithm (Random Forests) [22]. In the same year, Meineke et al. proved that ML could comprehensively detect chest CT investigations with dose optimization potential [51]. They used 3,199 CT chest exams for training and testing of different neural network layers and components, and the built model was improved and optimized and trained to predict the volumetric CT dose index (CTDIvol) based on scan patient metrics [51]. However, in the three previous works, the authors do not provide an architecture based on big data technologies and DL for dose optimization in cranial CT scanning for children.

Based on those cited works and to the best of our knowledge, none of the authors provide a specific pipeline and big data architecture to manage efficiency of cranial CT scan image for low dosage using DL, Spark framework, and MapReduce processing model. This drawback is the main interest of this paper. Indeed, we have designed a pipeline implementing a Fully CNN (FCNN) for processing CT scan image, and propose a method to split the biomedical image into sections before applying FCNN. Therefore, we can use the Spark framework and MapReduce programming and accelerate processing time with our proposed

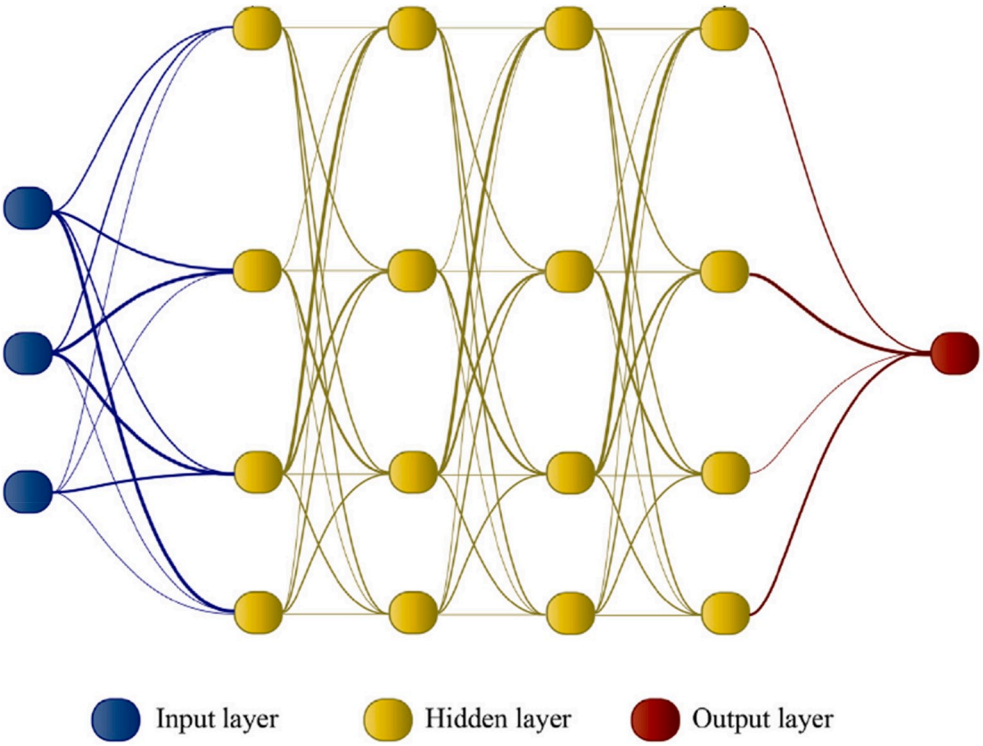

Fig. 2. Convolutional neural network (CNN) architecture.

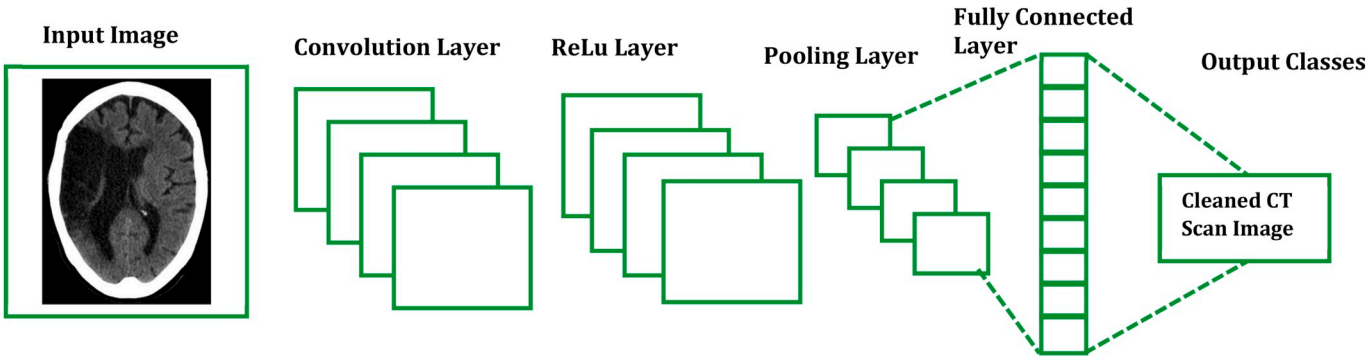

Fig. 3. Layers name for CT image denoising.

architecture. Our proposed architecture allows adapting low dosage in pediatric cranial CT imagery for a right diagnosis.

3. Methods

Many software and programming methods have been developed to segment imagery into many sections for processing. Indeed, dividing each image into sections, then processing them and consolidating is a typical process that is employed in many medical imaging pipelines. However, the new concept introduced in this paper is to perform parallel processing that is not actually done for a biomedical image. Whereas we divided each image into many sections traditionally, instead of processing each section one after another, we used the Spark framework to process many or all sections of an image simultaneously. Our proposed workflow is discussed in this section.

With the rising use of CT in modern medicine, concerns have arisen about an increasing radiation dosage to the community from biomedical imaging, and regarding the associated increasing estimated risk for radiation-induced cancer [52]. Optimization of the scanning methods is important, so that the necessary clinical information can be collected or captured with minimization of the radiation dose [53]. In this segment, we propose an optimal pipeline for low dosage CT image diagnosis based on CNN. Our proposed pipeline relies on four main parts: Captured image, Multi-Processing image, Denoising & Diagnosis, Share or Store. Fig. 1 shows the parts of our proposed pipeline.

3.1. Theory of image denoising in CT scanning

Image Denoising has remained a fundamental issue in the field of image processing [54]. Removing noise on originally captured image is still a challenging issue in digital image processing. Solving the details of an image and eliminating random noise as far as possible is the objective of image denoising approaches. Many denoising techniques depend on a mathematical approach. Mathematically, the problem of image denoising can be modelled in Refs. [55] by equation (1):

$$y = x + b \tag{1}$$

Where y is the observed noisy image, x is the unknown clean image, and b represents additive white Gaussian noise (AWGN) with standard deviation. In Ref. [54–58], the authors show that the image denoising techniques rely on the spatial domain (linear and non-linear) and transform domain (adaptive data transform and non-adaptive data transform). In this subsection, we introduce the denoising FCNN architecture applied in our work, which is based on work proposed in 2019 by Zhang et al. [59]. The process of updating parameters in the CNN architecture is presented in detail with a mathematical explanation. We address the CNN model for image denoising in this subsection.

In this part, we develop the mathematical model of CNN that allows us to predict a clean version from a noisy image based on CNN architecture and training processes. The CNN model has generally three layers, as presented in Fig. 2: input, hidden and output layers, respectively. However, we can group these three layers in two groups: Convolutional and Pooling operations, and Fully Connected Layer. On the other hand, these three layers are composed of a stack of operators which include the Dilated Convolution (DC) operator, the Batch Normalization (BN) operator and the Rectified Linear Unit (ReLu) [59, 60]. The ReLU plays the role of activation function. Fig. 3 presents the set of layers in a CNN architecture for image denoising.

- *Convolutional layer: Convolution operator;* In image analysis, convolution is defined as an operation on the input values (pixel values) at a position in the image and the second function is a filter (or kernel) [60,61]. The convolution operation is defined by the * symbol. An output (or feature map) $s(t)$ is defined below when input I (t) is convolved with a kernel $K(a)$ or filter.

$$s(t) = (I * K)(t) \tag{2}$$

The discretized convolution is given by equation (3) for the one-dimension operator, and when t takes only the integer values

$$s(t) = \sum_a I(a).K(t-a) \tag{3}$$

In this paper, we apply convolution in a CT Scan image (2D signal). The convolution operator for input image I (m, n) and a kernel K (a, b) is defined by (4):

$$s(t) = \sum_a I(a).K(t-a) \tag{4}$$

The kernel can be flipped using the commutative law, and equation (4) is rewritten by (5)

$$s(t) = \sum_a \sum_b I(m-a, n-b).K(a,b) \tag{5}$$

Neural networks implement the **cross-correlation** function, which is the same as convolution but without flipping the kernel [60,61].

$$s(t) = \sum_a \sum_b I(m+a, n+b).K(a,b) \tag{6}$$

- *DC Operator;* The DC function is defined in Ref. [62], and supports exponentially expanding receptive fields without losing resolution or coverage, and refers to a convolution with a dilate filter. The DC operator is defined by equations (1) and (2) in Ref. [62].

Consider F: $\mathbb{Z} \rightarrow \mathfrak{M}$to be a discrete function, and $\Omega_r = [-r, r]^2 \cap \mathbb{Z}^2$, $k : \Omega_r \rightarrow \mathfrak{M}$to be a discrete filter of size $(2r+1)^2$. The discrete convolution operator * can be defined by (7)

$$(F * k)(p) = \sum_{s+t=p} F(s)k(t) \tag{7}$$

Now consider l to be a dilation factor and $*l$ is defined by (8)

$$(F*_l k)(p) = \sum_{s*lt=p} F(s)k(t) \tag{8}$$

NB: This definition reflects the implementation of the DC operator, which does not involve construction of dilated filters.

- *Rectified Linear Unit (ReLu) Layer;* The ReLu layer is an activation function that sets negative input values to zero [60]. The ReLu helps to avoid the vanishing gradient problem, and simplifies and accelerates computation and training. Mathematically it is defined as:

$$f(x) = \max(0, x) \tag{9}$$

where x is the input to the neuron. Other activation functions include the tanh, leaky ReLu, sigmoid, parametric ReLu, and Randomized ReLu.

- *Pooling Layer;* to reduce the number of parameters to be calculated during implementation of the algorithm, the Pooling layer is inserted between the Convolution and RELU layers. Max-pooling is most commonly used because it simply takes the largest input value (image) within a filter and discards the other values; effectively it summarizes the strongest activations over a neighborhood [60,61].
- *BN Operator*; it is a differentiable transformation that introduces normalized activations into the network to ensure that as the model is training; layers can continue learning on input distributions that exhibit less internal covariate shift, thus accelerating the training [63]. Here, we normalize each scalar feature independently, by making it zero mean ($\mu_B = 0$) and unit variance ($\sigma_B^2 = 1$). During the training phase, we need to back propagate the gradient of loss through BN transformation, as well as compute the gradients with respect to some rule defined in Refs. [63] by equations (10)–(15).

$$\frac{\partial l}{\partial \widehat{x}_i} = \frac{\partial l}{\partial y_i} \times \gamma \tag{10}$$

$$\frac{\partial l}{\partial \sigma_B^2} = \sum_{i=1}^{m} \frac{\partial l}{\partial \widehat{x}_i} \times (x_i - \mu_B) \times \frac{-1}{2}\left(\sigma_B^2 + \varepsilon\right)^{-3/2} \tag{11}$$

$$\frac{\partial l}{\partial \mu_B} = \sum_{i=1}^{m} \frac{\partial l}{\partial \widehat{x}_i} \times \frac{-1}{\sqrt{\sigma_B^2 + \varepsilon}} \tag{12}$$

$$\frac{\partial l}{\partial x_i} = \frac{\partial l}{\partial \widehat{x}_i} \times \frac{1}{\sqrt{\sigma_B^2 + \varepsilon}} + \frac{\partial l}{\partial \sigma_B^2} \times \frac{2(x_i - \mu_B)}{m} + \frac{\partial l}{\partial \mu_B} \times \frac{1}{m} \tag{13}$$

$$\frac{\partial l}{\partial \gamma} = \sum_{i=1}^{m} \frac{\partial l}{\partial y_i} \times \widehat{x}_i \tag{14}$$

$$\frac{\partial l}{\partial \beta} = \sum_{i=1}^{m} \frac{\partial l}{\partial y_i} \tag{15}$$

where $\gamma, \beta$are the parameters to be learned, $B = \{x_1 \ldots\ldots x_m\}$represent m values of the training data set x;

$$y = \gamma\widehat{x} + \beta \Rightarrow y^{(k)} = \gamma^{(k)}\widehat{x}^{(k)} + \beta^{(k)}; \quad \gamma^{(k)} = \sqrt{\mathrm{var}[x^{(k)}]}; \quad \beta^{(k)} = E\left[x^{(k)}\right]$$

$\mu_B = \frac{1}{m}\sum_{i=1}^{m} x_i$ and $\sigma_B^2 = \frac{1}{m}\sum_{i=1}^{m}(x_i - \mu_B)^2$ represent the mean and variance of the mini-batch respectively. $\widehat{x}_i = \frac{x_i - \mu_B}{\sqrt{\sigma_B^2 + \varepsilon}}$ are normalized x parameters.

- *Fully Connected Layer; Updating the process of CNN parameters;* Stochastic gradient descent (SGD) has proven to be an effective way of training deep networks, and in optimizing parameters Θ of the network, so as to minimize loss [63]:

$$\Theta = \underset{\Theta}{\operatorname{argmin}} \frac{1}{m}\sum_{i=1}^{m} l(x_i, \Theta) \tag{16}$$

For CT Scan image denoising, we need to recover a clean image $\boldsymbol{x}$ from a noisy observation $\boldsymbol{y} = \boldsymbol{x} + \boldsymbol{b}$, where $\boldsymbol{b}$ denotes additive noise assumed to be Gaussian in function (see equation (1)). Here, as in Refs. [59], the CNN architecture based on residual learning is designed to learn the residual mapping $F(\boldsymbol{y}, \Theta)$to predict the residual noise $\boldsymbol{b}$, and $\boldsymbol{x} = \boldsymbol{y} - F(\boldsymbol{y}, \Theta)$is obtained as the CT Scan denoised image. Θ is considered as all trainable features in the CNN architecture. The minimized function of equation (16) can be rewritten by equation (17)

$$l(\Theta) = \frac{1}{2m}\sum_{i=1}^{m} \|F(y_i, \Theta) - (y_i - x_i)\|^2 \tag{17}$$

where $\{(y_i - x_i)\}_{i=1}^{m}$ represents m noisy-clean training pairs. By using the traditional backforward propagation, the loss is propagated from the last layer to the first layer through the rules defined in equations 10–15. The parameter $\theta_k \in \Theta$in the k-th layer is derived as:

$$\theta_k = \theta_k - \lambda\left(\frac{\partial l}{\partial \theta_k}\right) \tag{18}$$

where $\lambda$is the learning rate, and$\frac{\partial l}{\partial \theta_k}$ is acquired from the last layer to layer k by the chain rule.

The multi-processing step of Fig. 1 was based on many investigations provide by research in CT low dosage optimization using Deep CNN so as to propose our method [18,64–67]. The FCNN, which consists of multiple layers of neuron-like computational connections with minimal step-by-step processing, achieves significant improvements [68]. In this part, we can have two kinds of images, i.e., heavy and soft images. Indeed, some biomedical images are captured with a weight of two gigabytes or more, and others are less that one hundred megabytes. In our pipeline, if the input image is heavy, we divide it into many sections or subimages and use Spark with MapReduce based on FCNN to perform parallel processing of each subimage. At the end of processing, we use a table loop up to reconstruct the image. Thus, the reconstructed image is ready for the next stage. On the other side, for the soft image, we can use more than twenty images and process them also in Spark with FCNN using parallel programming. Use this processing method, we can obtain timesavings. In FCNN, each layer fully connects to the previous layer and spatial relationships are not necessarily preserved. However, training of FCNN is computationally demanding and requires large data sets that may not be readily available. Resolving the issue of training time that is generally high, a large community of machine learning engineers and programmers are dedicated to research and developing more versatile and faster software platforms for DL use cases. There are many examples such as Keras, TensorFlow, Pytorch, Theano, Torch, which provide an exciting experience and helpful interfaces to train and test deep learning architectures (DNN/CNN/FCNN) with fast and memory-efficient implementations [69–74]. Nowadays, almost every framework incorporates convolution, deconvolution, max pooling, fully connected, dropout techniques, and Batch Normalization, with many popular optimization methods implemented. Due to the lack of powerful computing, we propose in this paper an architecture based on DNN using Spark with MapReduce for parallel programming, to accelerate the CT low dosage image reconstruction. In this work, we build a cluster with one master and two slaves in order to reduce computing time. After the step of CT low dosage image reconstruction based on FCNN, we can move to the image diagnostic step of Fig. 1 where the specialist sees the new image and can make a diagnosis. Moreover, low dosage can be used to maintain patient health and safety. Based on our pipeline method, the specialist can provide a right diagnosis from the captured image. As explained in Ref. [6] Not Only SQL (NoSQL) technologies are nowadays an excellent database to store imagery (share or storage). Cloud computing technologies can also be used to facilitate sharing of data.

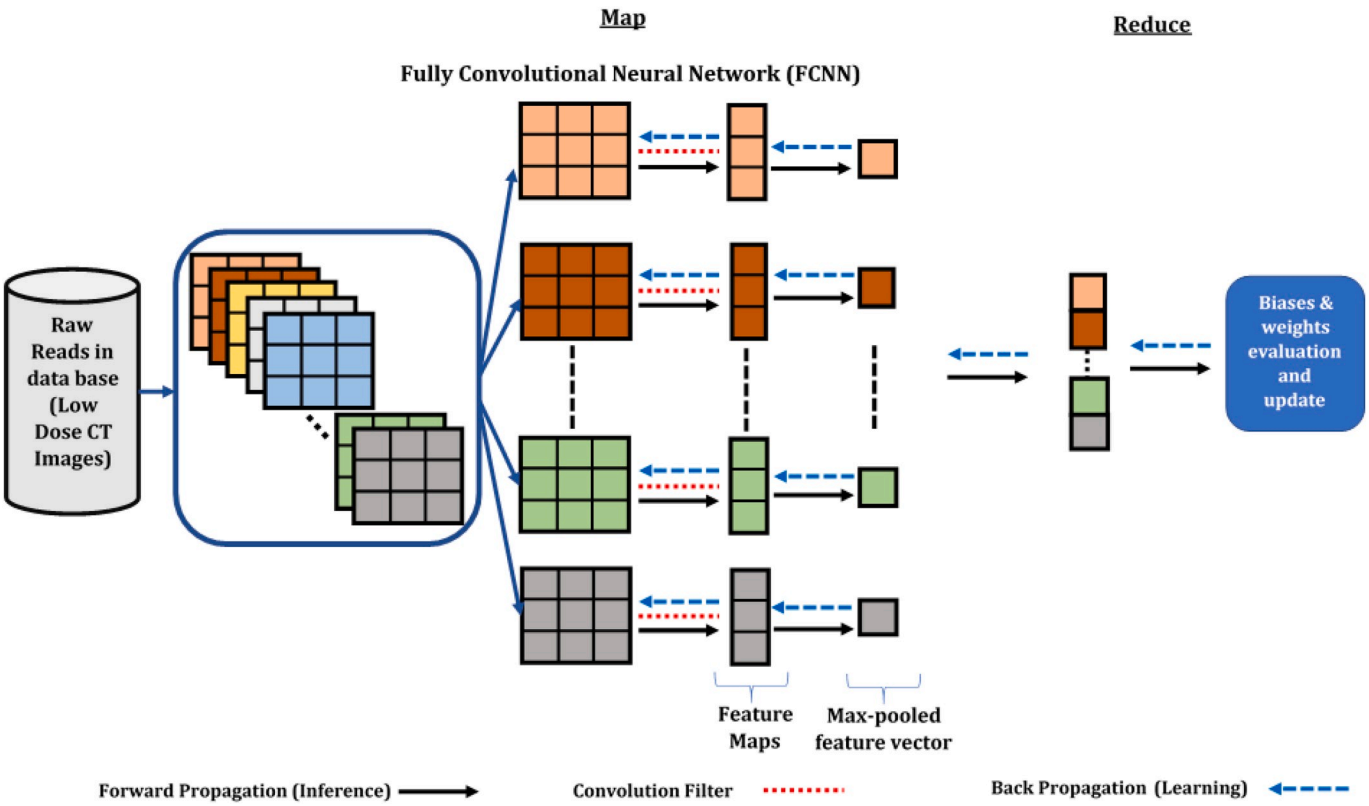

Fig. 4. Spark Map Reduce pipeline for low dose CT image reconstruction based on FCNN.

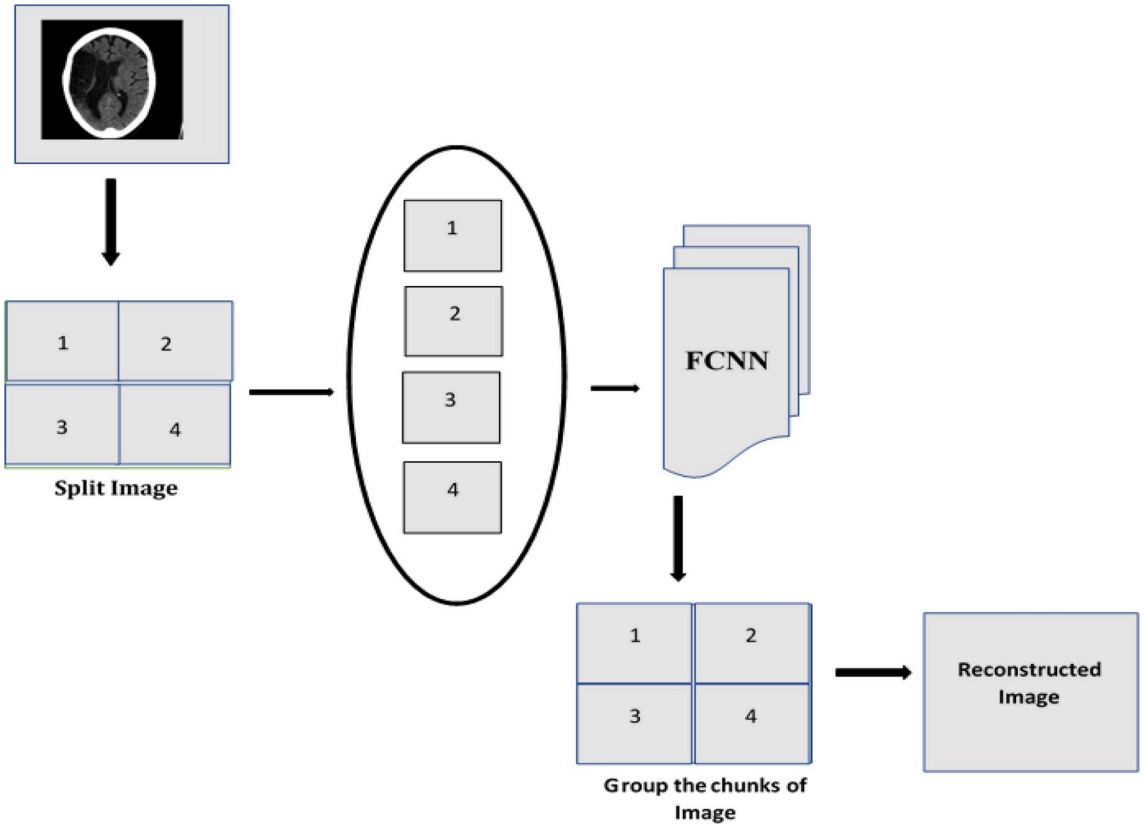

Fig. 5. Image processing pipeline into the proposed Spark architecture.

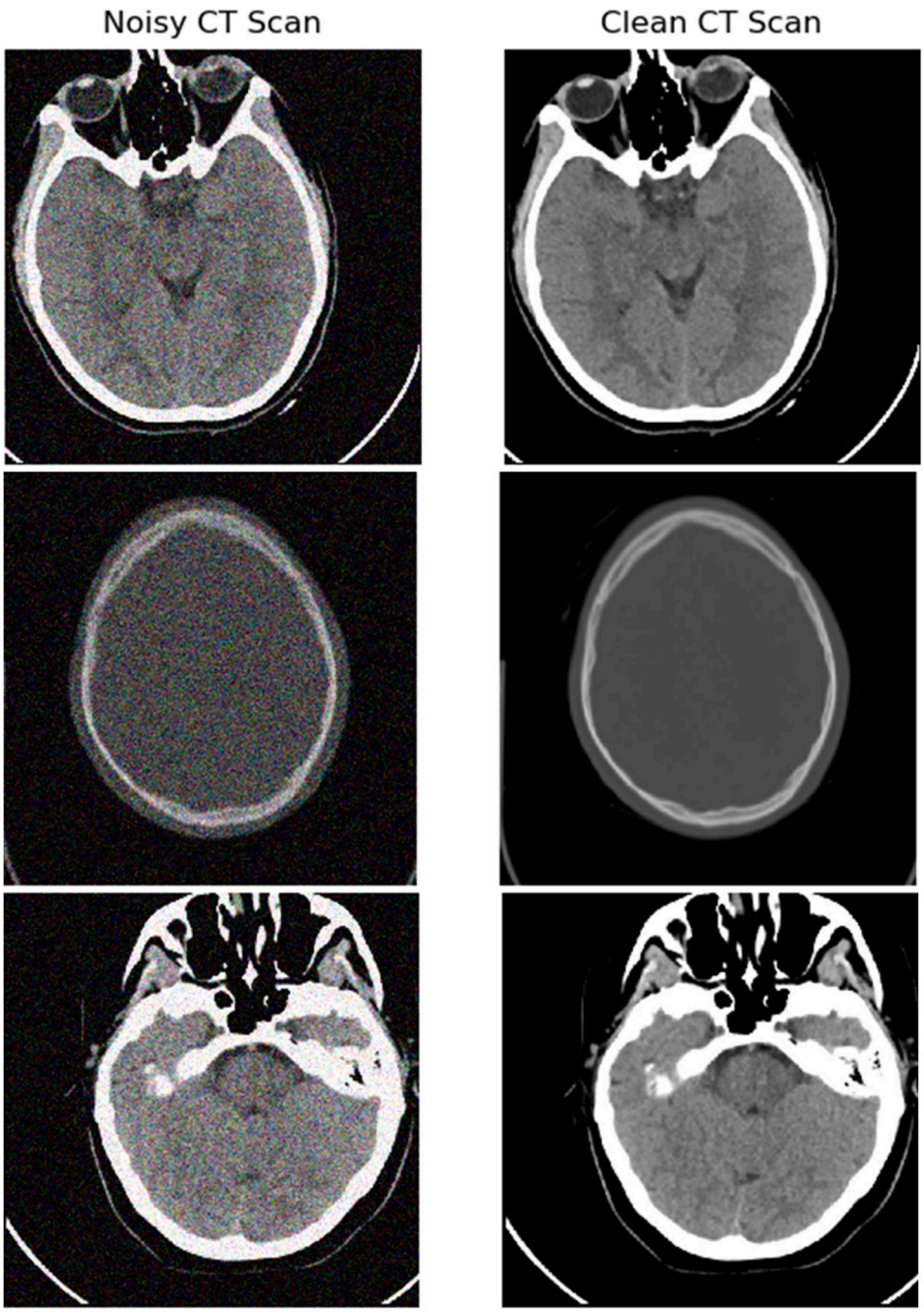

Fig. 6. Clean and noisy CT images.

Cloud computing is suited for big data bioinformatics applications, as it permits for on-demand provisioning of resources with a pay-as-you-go model, thus removing the need for purchasing and maintaining expensively local computing infrastructure to perform analyses and data processing [75]. Hence, in our pipeline, we can use a NoSQL database for storage and Cloud computing for sharing.

3.2. Proposed CT scan image denoising FCNN method

Development and Training of FCNN is still the subject of research. In the processing pipeline, we use DL for low dosage CT image reconstruction. In the next session, we design our optimal architecture using a best big data framework (Spark) with MapReduce to develop efficient and appropriate methods to process a low dose CT scanned image. In this subsection, we present the Spark architectures to handle the foremost step of the pipeline described in Fig. 1. The main goal of this architecture is to see how the CT image processes for reconstruction. Spark is based on MapReduce for parallel programming, and it extends with a data-sharing abstraction called Resilient Distributed Datasets (RDDs) [76]. Apache Spark is defined as a fast and general engine framework for large-scale data processing and managing. Spark is faster than previous approaches to work with Big Data including classical MapReduce or Hadoop, and is faster as it runs directly on Memory (RAM), which makes the processing much faster than to Disk [77].

The general part of Spark means that it can be used for multiple tasks, like creating data pipelines, running distributed SQL, ingesting data into a database, running ML algorithms, working with graphs, data streaming, and more [77]. Integration of the DL architecture as FCNN and

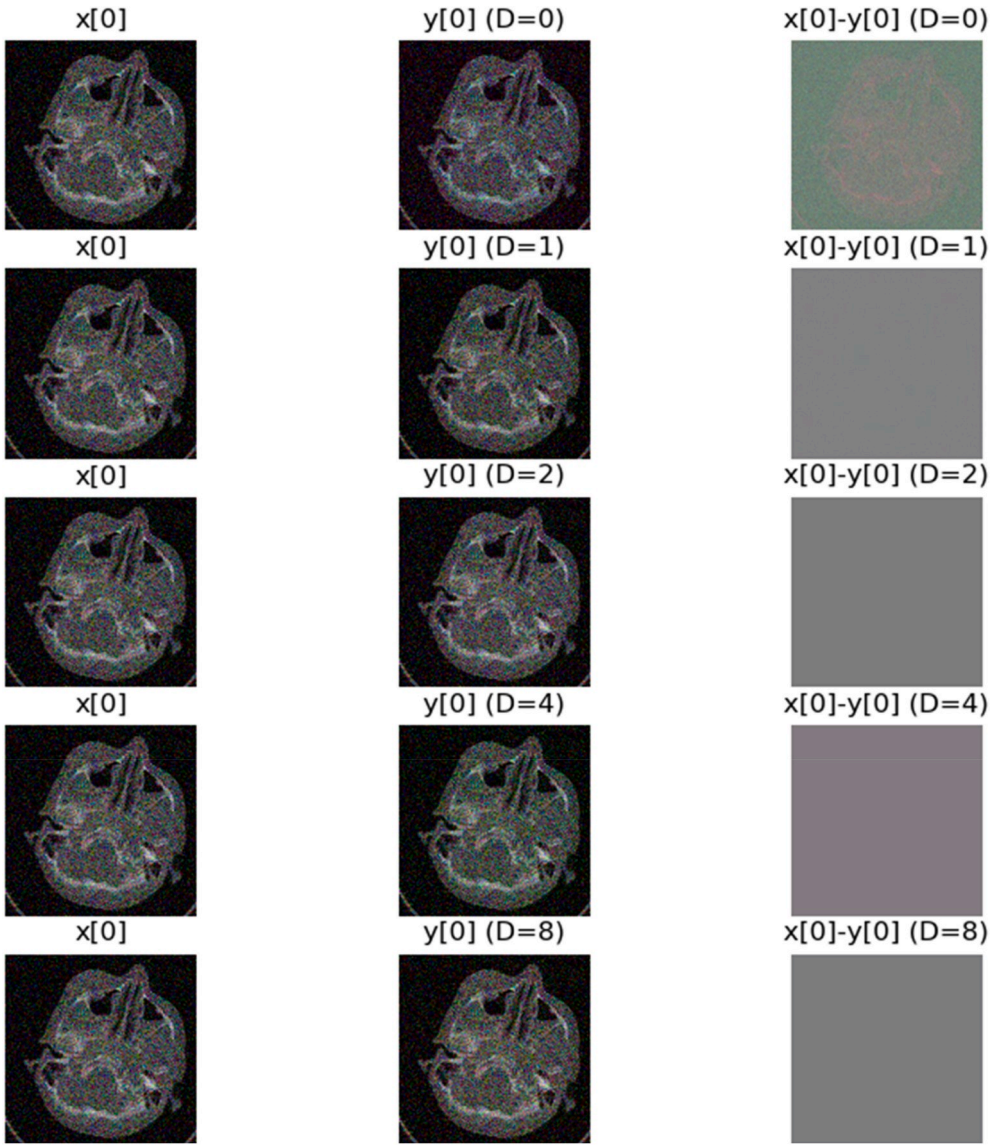

Fig. 7. FCNN without weight initialization.

Spark is a better solution to improve, optimize, and reduce the training time, and minimize the error rate of the DL model. DL from Spark has two main benefits: large-scale prediction and hyper-parameter tuning [78]. Also, the Spark Framework provides easy-to-use APIs that enable DL in very few lines of code from its Spark MLib library. Fig. 4 presents our Spark Architecture with FCNN for low dose CT image optimization. In this figure, we can see how the input image is trained using MapReduce programming and FCNN with backpropagation and forward propagation. We need to divide the image into a set of sections (with heavy imagery). The digital CT scanned image is commonly too large and therefore it increases the complexity of processing. To overcome this complexity, we split the image into many image segments and process each independently. By using a parallel programming method like MapReduce, we can perform the simultaneous process of these segments and thus reduce processing time as compared to traditional methods. Fig. 4 gives us an overview of how FCNN performs to reconstruct CT low dosage imagery into Spark. Indeed, the Spark architecture permits us to develop efficient and appropriate techniques to leverage a wide number of images. Fig. 5 presents an overview of image processing into Spark. Training our FCNN model on the Spark framework involves two main steps (MapReduce Programming) which occur iteratively and are repeated until the overall initialized error is sufficiently minimized:

- *Map Step*: the input data (Low dose CT images) are distributed across all nodes in the cluster, and each node trains the portion of the biomedical image data that it receives;
- *Reduce Step*: here, biases and weights across every node in the cluster are averaged together and each node updates the parameters of its own net with the new average value.

This scenario or concept allows us to process many CT images at the same time and optimize the processing time. Using the Spark framework, the process of dose optimization in pediatric cranial scanning using a DL architecture is complete, easier, and faster.

4. Results

In this section, the proposed architecture is based on Fig. 4 and we implement our algorithm for CT image denoising. Our goal is to use FCNN to learn equation (1) by minimizing the function of equation (17). We will consider the images from Kaggle [79] as our clean/ground-truth images: xi This dataset contains information for 37 female and 45 male patients; thus a total of 82 patients for 4615 CT images. However, we reduce the number of images due to the lack of computing power. Fig. 6 shows some of our noisy and clean images from the dataset. For each of

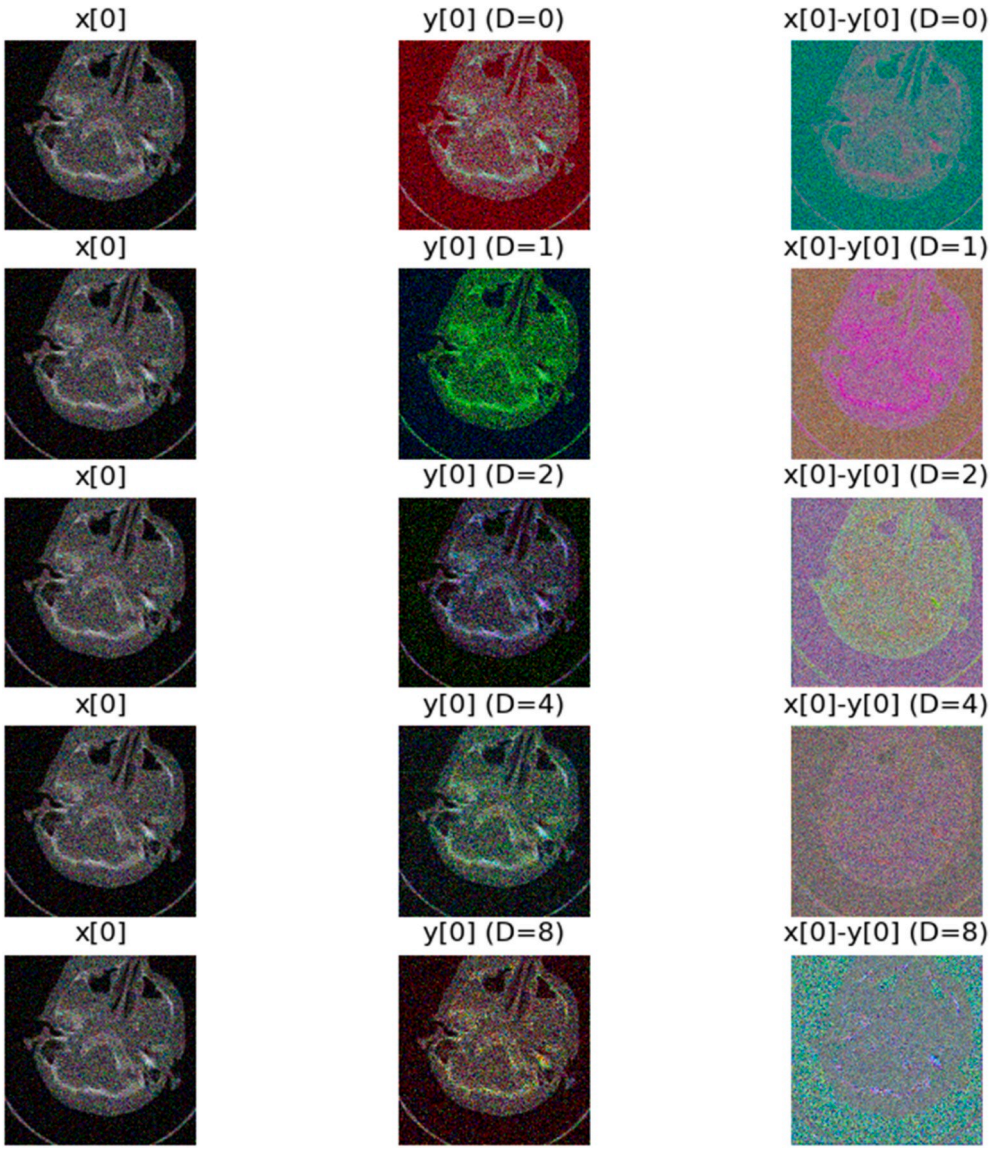

Fig. 8. FCNN with weight initialization.

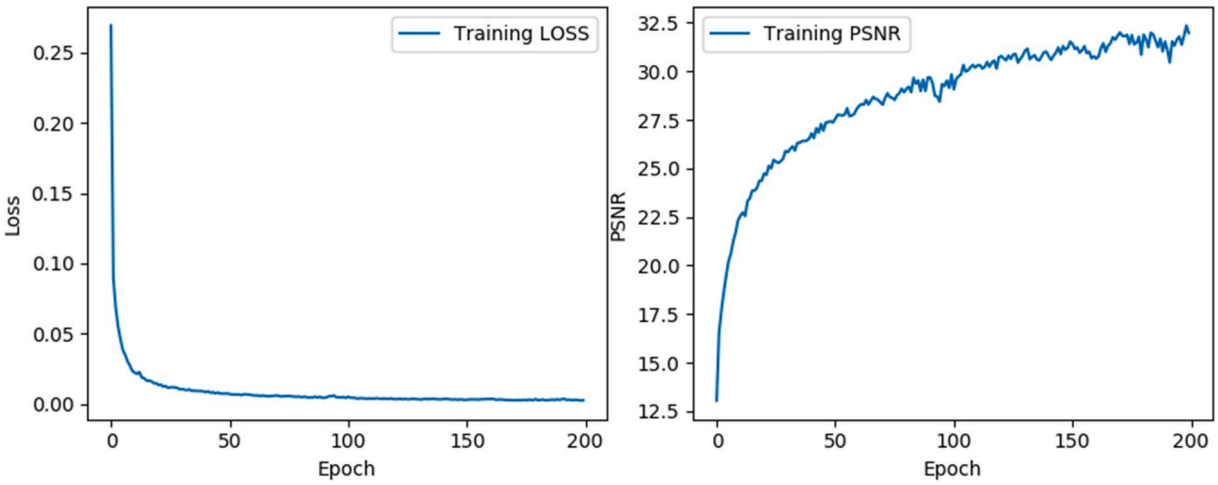

Fig. 9. Results of training model. (a) Training Loss (b) Training PSNR.

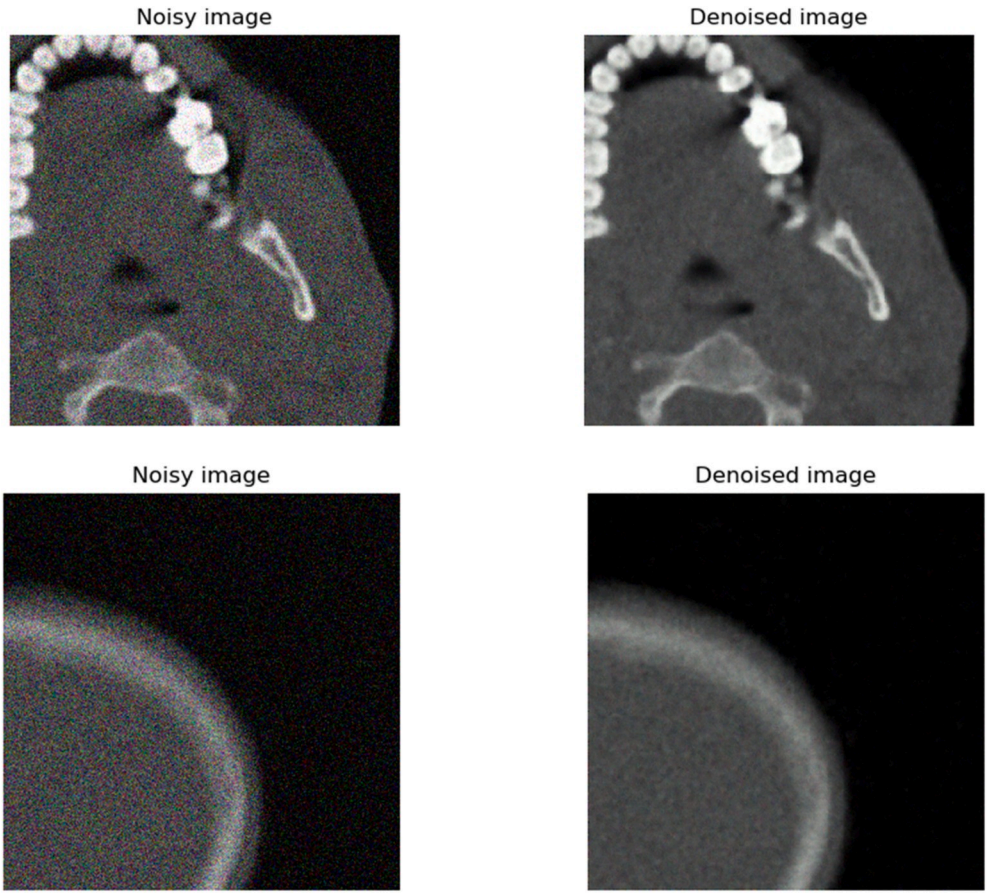

Fig. 10. Noisy Image and obtained image Denoising from our model.

them, we will generate noisy versions by adding white Gaussian noise: $yi = xi+bi$ (see equation (1)) where yi is a CT image with each pixel being an independent realization of a zero-mean Gaussian distribution with standard deviation $\sigma = 30$. Indeed, when we reduce the dose during CT scanning, the captured images are noisy and here we consider these noises as Gaussian distributed. Since CT images have different sizing, we will consider random crops of size of 180 × 180. As explained in Ref. [60,80], the weight initialization during the process of training our

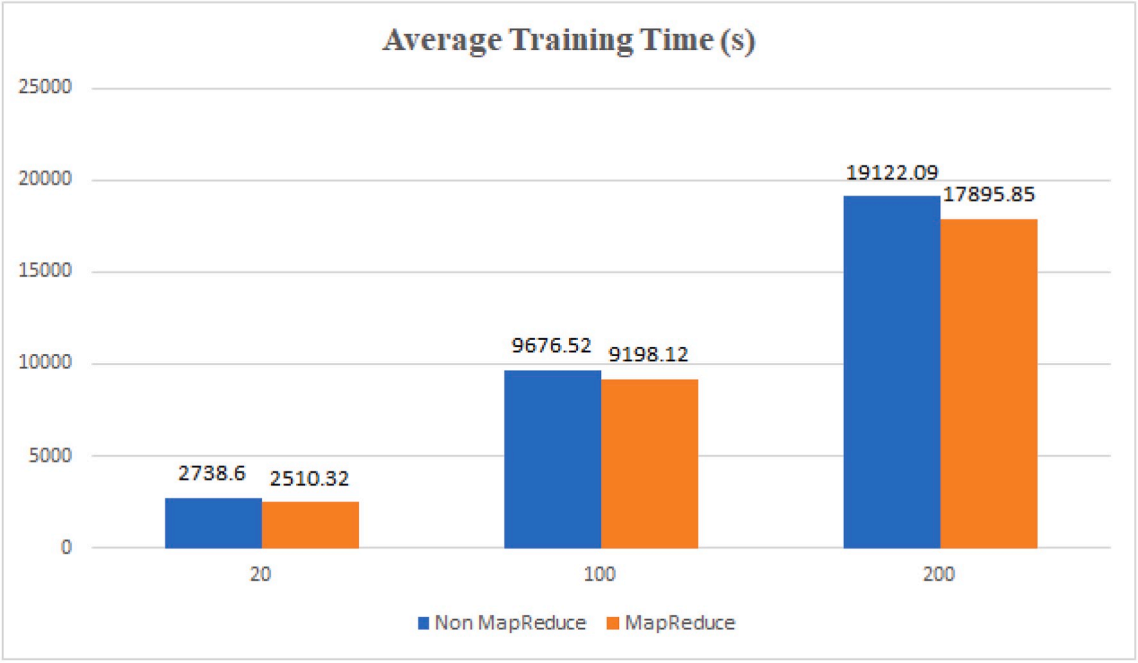

Fig. 11. Training time comparison: Non-MapReduce and MapReduce.

model is very important. Figs. 7 and 8 present examples of the image without and with weight initialization, respectively, according to the size of the dilated matrix D. In Fig. 7, except for FCNN with D = 0, the output of the network is like the input. In other words, their weighting and gradient update are the same as well, which means the network cannot learn properly. In Fig. 8, FCNN with different DC matrix have residuals with non-zero values because we avoid a vanishing gradient in the ReLu by initializing as activated half of the neurons. The output is now different from the input, and the weighting and gradient update are different, enabling the network to learn well. The training loss and training PSNR according to number of epochs are also presented in this section. The PSNR is defined in Ref. [12] by (19)

$$PSNR = 10\log_{10}\left(\frac{255^2}{MSE}\right) \tag{19}$$

Where

$$MSE = \frac{1}{M \times N}\sum_{i=0}^{M-1}\sum_{j=0}^{N-1}(x(i,j) - y(i,j))^2 \tag{20}$$

The PSNR gives an objective measure of distortion; the higher PSNR (greater than 30 dB) equals a good quality of image [12,81]. Fig. 9**a** and **b** present the Training Loss and the Training PSNR according to several epochs, respectively. We notice that in Fig. 9a, the Training loss is approaches 0.001; this shows the efficacy of our training model, and the training PSNR is close to 32 dB (Fig. 9. b). Hence, our DL method allows denoising of the CT scan image with good efficacy. This efficacy can be seen in Fig. 10 where we present the noisy and denoised image. To implement this work, we use a computer with Ubuntu OS, Spark, and work locally in one cluster that we built with one node. We store our images in MongoDB NoSQL. Fig. 11 shows the training time. Indeed, we represented the training time obtained for MapReduce and Non-MapReduce according to the number of epochs. We notice in this figure that the training time using MapReduce is slightly shorter than the training time with Non-MapReduce. This can explain that using MapReduce with one node allows the computer to be more powerfully used, but still insufficient. When the number of clusters and nodes increases, the training time reduces considerably. Due to the limited power of our computer, we haven't implemented a multi-node cluster.

5. Discussion

Advances in computer technology, GPU technology, and automated imaging platforms have transformed the field of biomedical image research. Today, new pipelines, workflows, and architectures are often proposed to improve this field. This work proposed a pipeline based on the FCNN and Spark Framework for CT low dose image reconstruction. The novelty of our pipeline is that it provides the optimal methods, techniques, and algorithms to use in each design stage. By using the characteristics of MapReduce, we can perform parallel processing in our proposed architecture. Based on the observations in the previous section, our proposed pipeline and architecture provide low dose optimization in biomedical imaging. They can be customized and adapted in other biomedical applications. To see the efficiently of our proposed architecture, we compared it with another architecture described in the literature. In Ref. [13], the authors also proposed an FCNN architecture for CT low dose optimization. However, their architecture is not based on the Spark framework and cannot process many images at the same time. As in Ref. [13] we propose two main steps for training: forward propagation where the low-quality image is passed through the network and the output is acquired by calculating a set of convolutions. And back-propagation where the derivative of the loss function with respect to every network parameter is calculated, and these values are updated using the calculated gradient to decrease the loss. Also, in Ref. [82], the author design was based on a plug-and-play Framework and a DL architecture for CT reconstruction and they obtained a good result. Despite this, the authors do not use the DL for low dose reconstruction. They are used only for image denoising. As presented in session 2, they have not shown in the literature reliance on a Spark framework using DL for CT low dose reconstruction. The ability to easily adapt our proposed architecture can be useful to modify or improve the processing systems available in healthcare. Our pipeline is based on the NoSQL database and can support structured and unstructured biomedical images formatting including the DICOM format and other commonly used formats. Our pipeline gives us another aspect to use cloud computing to manage our biomedical images. The implementation of this work was done by using one cluster with one node. It will be interesting to perform an implementation in one cluster with multi-node and also a multi-node cluster. This can reduce considerably the training time to build our model, and we can also increase the epochs to improve to quality of our model.

6. Conclusion

Deep Learning has shown promising results in clinical studies, as it allows significant reconstruction during dose reduction CT scanning while maintaining a useful diagnostic. In this paper, we outlined some important research in the field of low dose CT optimization, and the low dose CT reconstruction problem has been investigated from a DL point of view. We proposed a pipeline for low dose image reconstruction using FCNN into the Spark framework. To design our pipeline, we conducted a literature review to identify the most suitable methods for CT low dose image optimization. Thus, we were able to provide for each stage of our pipeline, a method to obtain an optimal architecture. To overview our proposed methods, we designed a Spark architecture for low dose CT reconstruction using FCNN. The obtained results show the efficacy and efficiency of our proposed method. The denoising performance of the model is greatly affected by training data, which is a common problem in discriminative learning methods. In the future, we will construct our own dataset to improve the processing of CT scan image denoising and implement our algorithm in a multi-node cluster.

Funding and competing interests

We wish to confirm that there are no known conflicts of interest associated with this publication, and there has been no significant financial support for this work that could influence its outcome.

Ethical approval

This article does not contain any studies with human participants and/or animals performed by any of the authors.

Acknowledgements

The authors are very grateful to the anonymous referees for their valuable comments which helped to improve the quality of the paper. The authors would like to acknowledge both Pr. Geugang Emilienne from Service de Radiologie et d'Imagerie Médicale, Hôpital Général de Yaoundé-Cameroun, and the InchTech's (www.inchtechs.com) Team for their support and assistance during the conception of this work.

References

[1] Lakhani P, Prater AB, Hutson RK, et al. Machine learning in Radiology: applications beyond image interpretation. J Am Coll Radiol 2018;15:350–9. https://doi.org/10.1016/j.jacr.2017.09.044.

[2] Kim J, Hong J, Park H. Prospects of deep learning for medical imaging. Precision Future Med 2018;2(2):37–52. https://doi.org/10.23838/pfm.2018.00030.

[3] Wang W, Zhang M, Chen G, Jagadish HV, Ooi BC, Tan KL. Database meets deep learning: challenges and opportunities. SIGMOD Record 2016;45(2):17–22.

[4] You C, Li G, Zhang Y, et al. CT super-resolution GAN constrained by the identical, residual, and cycle learning ensemble (GAN-CIRCLE). IEEE Transact. Med. Imag. 2020;39(1):188–220. asarXiv:1808.04256v3.

[5] Yoo J, Sabir S, Heo D, et al. Deep Learning Can Reverse Photon Migration for Diffuse Optical Tomography. 2017. arXiv:1712.00912v1.

[6] Tchagna Kouanou A, Tchiotsop D, Kengne R, Djoufack Tansaa Z, Ngo Moelas AA, Tchinda R. An optimal big data workflow for biomedical image analysis. Elsevier Informat Med Unlocked 2018;11:68–74. https://doi.org/10.1016/j.imu.2018.05.001.

[7] Chmelik J, Jakubicek R, Walek P. Deep convolutional neural network-based segmentation and classification of difficult to define metastatic spinal lesions in 3D CT data. Elsevier Med Image Anal 2018;49:76–88. https://doi.org/10.1016/j.media.2018.07.008.

[8] Gao XW, Hui R, Tian Z. Classification of CT brain images based on deep learning networks. Comput Methods Programs Biomed 2016. https://doi.org/10.1016/j.cmpb.2016.10.007. https://search.crossref.org/?q=Gao+XW%2C+Hui+R%2C+Tian+Z%2C+Classification+of+CT+brain+images+based+on+deep+learning+networks%2C+Computer+Methods+and+Programs+in+Biomedicine+%282016%29.

[9] Sandfort V, Choi Y, Symons R, Chen MY, Bluemke DA. An optimized test bolus contrast injection protocol for consistent coronary artery luminal enhancement for coronary CT angiography. Acad Radiol 2019;27:371–80. https://doi.org/10.1016/j.acra.2019.05.003.

[10] Schindler P, Kehl HG, Wildgruber M, Heindel W, Sch€ulke C. Cardiac CT in the preoperative diagnostics of neonates with congenital heart disease: radiation dose optimization by omitting test bolus or bolus tracking. Acad Radiol 2019;1–7. https://doi.org/10.1016/j.acra.2019.07.019.

[11] Fan R, Shi X, Yi Q, Yun W, Li F, Rutan C, Yi X, Liu S. Optimized categorization algorithm of coronary artery calcification score on non-gated chest low-dose CT screening using iterative model reconstruction technique. Jct 2018. https://doi.org/10.1016/j.clinimag.2018.08.015.

[12] Tchagna Kouanou A, Tchiotsop D, Tchinda R, et al. A machine learning algorithm for biomedical images compression using orthogonal transforms. Int J Image, Graphics and Signal Process (IJIGSP) 2018;10:38–53. https://doi.org/10.5815/ijigsp.2018.11.05.

[13] Bazrafkan S, Nieuwenhove VV, Soons J, Beenhouwer JD, Sijbers J. Deep Learning Based Computed Tomography Whys and Wherefores. 2019. arXiv:1904.03908v1.

[14] Papadimitroulas P, Kostou T, Chatzipapas K, et al. A review on personalized pediatric dosimetry applications using advanced computational tools. IEEE Trans Radiat Plasma Med Sci 2018. https://doi.org/10.1109/TRPMS.2018.2876562.

[15] Chen H, Zhang Y, Kalra MK et al., Low-dose CT with a residual encoder-decoder convolutional neural network (RED-CNN), IEEE Trans Med Imag, DOI 10.1109/TMI.2017.2715284.

[16] Pehrson LM, Nielsen MB, Lauridsen CA. Automatic pulmonary nodule detection applying deep learning or machine learning algorithms to the LIDC-IDRI database: a systematic review. MDPI Diagn. 2019;9:29. https://doi.org/10.3390/diagnostics9010029.

[17] Arbabshirani MR, Fornwalt BK, Mongelluzzo GJ. Advanced machine learning in action: identification of intracranial hemorrhage on computed tomography scans of the head with clinical workflow integration. NPI Digital Med 2018;1:9. https://doi.org/10.1038/s41746-017-0015-z.

[18] Lou B, Doken S, Zhuang T. An image-based deep learning framework for individualising radiotherapy dose: a retrospective analysis of outcome prediction. Elsevier Lancet Digit Health 2019;1:e136–47.

[19] Klimont M, Flieger M, Rzeszutek J, Stachera j, Zakrzewska A, JoNczyk-Potoczna K. Automated ventricular system segmentation in paediatric patients treated for hydrocephalus using deep learning methods. Hindawi BioMed Res Int 2019;3059170:9p. https://doi.org/10.1155/2019/3059170.

[20] Landers A, Neph R, Scalzo F, Ruan D, Sheng K. Performance comparison of knowledge-based dose prediction techniques based on limited patient data. Technol Canc Res Treat 2018;17:1–10. https://doi.org/10.1177/1533033818811150.

[21] Kim T, Heo J, Jang DK, et al. Machine learning for detecting moyamoya disease in plain skull radiography using a convolutional neural network. Elsevier EBioMedicine; 2018. https://doi.org/10.1016/j.ebiom.2018.12.043.

[22] Gu P, Jiang C, Ji M, et al. Low-dose computed tomography image super-resolution reconstruction via random forests. Sensors 2019;19:207. https://doi.org/10.3390/s19010207.

[23] Papadimitroulas P, Kostou T, Chatzipapas K, et al. A review on personalized pediatric dosimetry applications using advanced computational tools. IEEE Trans Radiat Plasma Med Sci 2018. https://doi.org/10.1109/TRPMS.2018.2876562.

[24] Rensselaer Polytechnic Institute. Machine learning approach for low-dose CT imaging yields superior results: Findings make a strong case for harnessing the power of artificial intelligence in CT, ScienceDaily. ScienceDaily. 10 June 2019. www.sciencedaily.com/releases/2019/06/190610111505.htm. [Accessed 11 August 2019].

[25] Serna A, Ramos D, Garcia-Angosto E. Optimization of CT protocols using cause-and-effect analysis of outliers. Phys Med 2018;55:1–7. https://doi.org/10.1016/j.ejmp.2018.10.010.

[26] Hedgire S, Ghoshhajra, Kalra M, et al. Dose optimization in cardiac CT. Phys Med 2017. https://doi.org/10.1016/j.ejmp.2017.04.021.

[27] Mhaylov IB, Moros EG. Integral dose based inverse optimization objective function promises lower toxicity in head-and-neck. Phys Med 2018;54:77–83. https://doi.org/10.1016/j.ejmp.2018.06.635.

[28] Martini K, Moona JW, Revel MP. Optimization of acquisition parameters for reduced-dose thoracic CT: A phantom study, Diagnostic and Interventional Imaging. 2020. https://doi.org/10.1016/j.diii.2020.01.012.

[29] Cubillos-Mesías M, Troost EGC, Lohaus F, et al. Including anatomical variations in robust optimization for head and neck proton therapy can reduce the need of adaptation. Radiother Oncol 2019;131:127–34. https://doi.org/10.1016/j.radonc.2018.12.008.

[30] Goenka AH, Dong F, Wildman B, et al. CT Radiation Dose Optimization and Tracking Program at a Large Quaternary-Care Health Care System. American College of Radiology; 2015. https://doi.org/10.1016/j.jacr.2015.03.037.

[31] Trattner S, Pearson GDN, Chin C, et al. Standardization and Optimization of CT Protocols to Achieve Low Dose American College of Radiology. 2014. https://doi.org/10.1016/j.jacr.2013.10.016.

[32] Miglioretti DL, Johnson E, Williams A. The use of computed tomography in pediatrics and the associated radiation exposure and estimated cancer risk. JAMA Pediatr 2013;167(8):700–7. https://doi.org/10.1001/jamapediatrics.2013.311.

[33] Mao T, Cuadros AP, Ma X, He W, Chen Q, Arce GR. Fast optimization of coded apertures in X-ray computed tomography. Optic Express 2018;26(19):2261–78. https://doi.org/10.1364/OE.26.024461.

[34] Sakhnini L. CT radiation dose optimization and reduction for routine head, chest and abdominal CT examination. Radiol Diagn Imaging 2017;2(1):1–4. https://doi.org/10.15761/RDI.1000120.

[35] Parakh A, Kortesniemi M, Schindera ST, CT Radiation Dose Management. A comprehensive optimization process for improving patient safety. Radiology 2016;280(3):663–73. https://doi.org/10.1148/radiol.2016151173.

[36] Dalmazo J, Júnior JE, Brocchi MAC, Costa PR, Azevedo-Marques PM. Radiation dose optimization in routine computed tomography: a study of feasibility in a University Hospital. Radiol Bras 2010;43(4):241–8.

[37] Dougeni E, Faulkner K, Panayiotakis G. A review of patient dose and optimisation methods in adult and paediatric CT scanning. Elsevier Eur J Radiol 2012;81:e665–83. https://doi.org/10.1016/j.ejrad.2011.05.025.

[38] Smith-Bindman R, Wang Y, Chu P, et al. International variation in radiation dose for computed tomography examinations: prospective cohort study. BMJ 2019;364:k4931. https://doi.org/10.1136/bmj.k4931.

[39] Abdulkadir MK, Yusra Mat Rahim NA, Mazlan NS, Daud NM, Shuaib IL, Osman ND. Dose optimisation in paediatric CT examination: assessment on current scanning protocols associated with radiation dose. Radiat Phys Chem 2020. https://doi.org/10.1016/j.radphyschem.2020.108740.

[40] Choi HR, Kim RE, Heo CW, Kim CW, Yoo MS, Lee Y. Optimization of dose and image quality using self-produced phantom with various diameters in pediatric abdominal CT scan. Optik 2018;168:54–60. https://doi.org/10.1016/j.ijleo.2018.04.066.

[41] Tozakidou M, Yang SR, Kovacs BK, et al. Dose-optimized computed tomography of the cervical spine in patients with shoulder pull-down: is image quality comparable with a standard dose protocol in an emergency setting? Eur J Radiol 2019;120:108655. https://doi.org/10.1016/j.ejrad.2019.108655.

[42] Chen GP, Noid G, Tai A, et al. Improving CT quality with optimized image parameters for radiation treatment planning and delivery guidance. Phys Imaging Radiat Oncol 2017;4:6–11. https://doi.org/10.1016/j.phro.2017.10.003.

[43] Kang E, Min J, Ye JC. A deep convolutional neural network using directional wavelets for low-dose X-ray CT reconstruction. Med Phys 2017;44(10):e330–7.

[44] Jung KH, Park H, Hwang W. Deep learning for medical image analysis: applications to computed tomography and magnetic resonance imaging. Hanyang Med Rev 2017;37:61–70. https://doi.org/10.7599/hmr.2017.37.2.61.

[45] Xuy J, Gongy E, Pauly J, Zaharchuk G. 200x Low-dose PET Reconstruction using Deep Learning. 2017. arXiv:1712.04119v1.

[46] Liu P, Wang M, Wang Y, et al. Impact of deep learning-based optimization algorithm on image quality of low-dose coronary CT angiography with noise reduction: a prospective study. Acad Radiol 2019:1–8. https://doi.org/10.1016/j.acra.2019.11.010.

[47] Wurfl T, Hoffmann M, Christlein V, et al. Deep learning computed tomography: learning projection-domain weights from image domain in limited angle problems. IEEE Trans Med Imag 2018. https://doi.org/10.1109/TMI.2018.2833499.

[48] Shan H, Zhang Y, Yang Q, et al. 3D convolutional encoder-decoder network for low-dose CT via transfer learning from a 2D trained network. IEEE Trans Med Imag 2018. https://doi.org/10.1109/TMI.2018.2832217.

[49] Tian C, Xu Y, Zuo W. Image denoising using deep CNN with batch renormalization. Neural Network 2020;121:461–73. https://doi.org/10.1016/j.neunet.2019.08.022.

[50] Lee H, Kim M and Do S, Practical Window Setting Optimization for Medical Image Deep Learning, Machine Learning for Health (ML4H) Workshop at NeurIPS 2018. arXiv:1812.00572v1.

[51] Meineke A, Rubbert C, Sawicki LM, Thomas C, et al. Potential of a machine-learning model for dose optimization in CT quality assurance. Springer Eur Radiol 2019;9p. https://doi.org/10.1007/s00330-019-6013-6.

[52] Singh S, Kalra MK, Moore MA. Dose reduction and compliance with pediatric CT protocols adapted to patient size, clinical indication, and number of prior studies. Radiology 2009;252(1):200–8. https://doi.org/10.1148/radiol.2521081554.

[53] Ferrero A, Takahashi N, Vrtiska TJ, et al. Understanding, justifying, and optimizing radiation exposure for CT imaging in nephrourology. Nat Rev Urol 2019;16(4):231–44. https://doi.org/10.1038/s41585-019-0148-8.

[54] Motwani MC, Gadiya MC, Motwani RC. Survey of image denoising techniques. https://www.cse.unr.edu/~fredh/papers/conf/034-asoidt/paper.pdf.

[55] Fan L, Zhang F, Fan H, Zhang C. Brief review of image denoising techniques. Springer Vis Comput Ind, Biomed Art 2019;2:7. https://doi.org/10.1186/s42492-019-0016-7.

[56] Huang H-M, Lin C. A kernel-based image denoising method for improving parametric image generation. Elsevier Med Image Anal 2019;55:41–8. https://doi.org/10.1016/j.media.2019.04.003.

[57] Mohana J, Krishnavenib V, Guo Y. A survey on the magnetic resonance image denoising methods. Elsevier Biomed Signal Process Control 2014;9:56–69. https://doi.org/10.1016/j.bspc.2013.10.007.
[58] Zhang X-W, Lei Zhu L, Zheng X-B. Study to the image denoising algorithm based on multiwavelet transforms. IEEE Int Conf Wavelet Anal Pattern Recogn 2007. https://doi.org/10.1109/ICWAPR.2007.4421746.
[59] Zhang Y, Lin H, Li Y, Ma H. A patch based denoising method using deep convolutional neural network for seismic image. IEEE Access 2019;7:156883–94. https://doi.org/10.1109/ACCESS.2019.2949774.
[60] Deisenroth MP, Faisal AA, Ong CS. Mathematics for Machine Learning. Cambridge University Press; 2020. p. 417p.
[61] Ker J, Wang L, Rao J, Lim T. Deep learning applications in medical image analysis. IEEE Access 2018;6:9375–89. https://doi.org/10.1109/ACCESS.2017.2788044.
[62] Yu F, Koltun V. Multi-scale context aggregation by dilated convolutions. In: Proc. Int. Conf. Learn. Represent. ICLR); 2016. p. 1–13.
[63] Ioffe S, Szegedy C. Batch normalization: accelerating deep network training by reducing internal covariate shift. Proc Int Conf Mach Learn 2015:448–56.
[64] Park J, Huang D, Kim KY, Kang SK, Kim YK, Lee JS. Computed tomography super-resolution using deep convolutional neural network. IOP Phys Med Biol 2018;63 (13pp):145011. https://doi.org/10.1088/1361-6560/aacdd4.
[65] Liang K, Yang H, Xing Y. Comparison of projection domain, image domain, and comprehensive deep learning for sparse-view X-ray CT image reconstruction. 2019. arXiv:1804.04289v2.
[66] Chen H, Zhang Y, Zhang W, et al. Low-dose CT via convolutional neural network. Biomed Optic Express 2017;8(2):679–94. https://doi.org/10.1364/BOE.8.000679.
[67] Lu L, Wang X, Carneiro G, Yang L. Deep learning and convolutional neural networks for medical imaging and clinical informatics. Springer Nat Switz 2019; 452p. https://doi.org/10.1007/978-3-030-13969-8.
[68] Lee J-G, Jun S, Cho Y-W, et al. Deep learning in medical imaging: general overview. Kor J Radiol 2017;18(4):570–84. https://doi.org/10.3348/kjr.2017.18.4.570.
[69] Abadi M, Barham P, Chen J, Chen Z, Davis A, Dean J, et al. TensorFlow: a system for large-scale machine learning. OSDI 2016;16:265–83.
[70] Gulli A, Pal S. Deep Learning with Keras: Implement neural networks with Keras on Theano and TensorFlow. Birmingham: Packt Publishing; 2017. p. 490p.
[71] Fu Y, Aldrich C. Using convolutional neural networks to develop state-of-the-art flotation froth image sensors. Elsevier IFAC-Papers OnLine 2018;51(21):152–7.
[72] Bergstra J, Bastien F, Breuleux O, Lamblin P, Pascanu R, et al. Theano: Deep learning on gpus with python, NIPS 2011, BigLearning Workshop, vol. 3. Granada, Spain: Citeseer; 2011.
[73] Paszke A, Chintala S, Collobert R, Kavukcuoglu K, Farabet C, et al. Pytorch: Tensors and dynamic neural networks in python with strong gpu acceleration. 2017.
[74] Gibson E, Li W, Sudre C, Fidon L, et al. NiftyNet: a deep-learning platform for medical imaging. Elsevier Comput Methods Progr Biomed 2018;158:113–22. https://doi.org/10.1016/j.cmpb.2018.01.025.
[75] Yang A, Troup M, Ho JWK. Scalability and validation of big data bioinformatics software. Comput Struct Biotechnol J 2017;8. Article in press.
[76] Zaharia M, Xin RS, Wendell P, et al. Apache Spark: a unified engine for big data processing. Commun ACM 2016;59(11):56–65. https://doi.org/10.1145/2934664.
[77] Vazquez F. Deep learning with Apache Spark (assessed on 02/09/2019), https://towardsdatascience.com/deep-learning-with-apache-spark-part-1-6d397c16abd.
[78] Venkatesan NJ, Nam C, Shin DR. Deep Learning Frameworks on Apache Spark: A Review. IETE Technical Review; 2018. https://doi.org/10.1080/02564602.2018.1440975.
[79] CT scan image dataset. https://www.kaggle.com/vbookshelf/computed-tomography-ct-images/. [Accessed 19 February 2020].
[80] Dolezel P, Skrabanek P, Gago L. Weight initialization possibilities for feedforward neural network with linear saturated activation functions. IFAC-PapersOnLine 2016;49–25. https://doi.org/10.1016/j.ifacol.2016.12.009. 049–054.
[81] Tchagna Kouanou A, Tchiotsop D, Fozin Fonzin T, Mounmo Bayangmbe, Tchinda R. Real-time image compression system using an embedded board. Sci J Circ Syst Signal Process 2019;7(4):81–6. https://doi.org/10.11648/j.cssp.20180704.11.
[82] Ye DY, Srivastava S, Thibault JB, Hsieh J, Sauer K, Bouman C. Deep residual learning for model-based iterative CT reconstruction using plug-and-play framework. https://doi.org/10.1109/icassp.2018.8461408.